Transgenic Expression of Constitutively Active RAC1 Disrupts Mouse Rod Morphogenesis

Hongman Song,[1] Ronald A. Bush,[1] Camasamudram Vijayasarathy,[1] Robert N. Fariss,[2] Sten Kjellstrom,[*,1] and Paul A. Sieving[1,3]

[1]Section for Translational Research in Retinal and Macular Degeneration, National Institute on Deafness and Other Communication Disorders, National Institutes of Health, Bethesda, Maryland, United States
[2]Biological Imaging Core Facility, National Eye Institute, National Institutes of Health, Bethesda, Maryland, United States
[3]National Eye Institute, National Institutes of Health, Bethesda, Maryland, United States

Correspondence: Paul A. Sieving, BG 31, RM6A03, 31 Center Drive, Bethesda, MD 20892, USA; paulsieving@nei.nih.gov.

Current affiliation: *Department of Ophthalmology, Lund University, Sweden.

Submitted: November 20, 2013
Accepted: March 10, 2014

Citation: Song H, Bush RA, Vijayasarathy C, Fariss RN, Kjellstrom S, Sieving PA. Transgenic expression of constitutively active RAC1 disrupts mouse rod morphogenesis. *Invest Ophthalmol Vis Sci*. 2014;55:2659–2668. DOI:10.1167/iovs.13-13649

Purpose. Dominant-active RAC1 rescues photoreceptor structure in *Drosophila* rhodopsin-null mutants, indicating an important role in morphogenesis. This report assesses the morphogenetic effect of activated RAC1 during mammalian rod photoreceptor development using transgenic mice that express constitutively active (CA) RAC1.

Methods. Transgenic mice were generated by expressing CA RAC1 under control of the *Rhodopsin* promoter, and morphological features of the photoreceptors were evaluated by histology, immunohistochemistry, and transmission electron microscopy. Function was evaluated by electroretinography. Potential protein partners of CA RAC1 were identified by co-immunoprecipitation of retinal extracts.

Results. Constitutively active RAC1 expression in differentiating rods disrupted outer retinal lamination as early as postnatal day (P)6, and many photoreceptor cell nuclei were displaced apically into the presumptive subretinal space. These photoreceptors did not develop normal inner and outer segments and had abnormal placement of synaptic elements. Some photoreceptor nuclei were also mislocalized into the inner nuclear layer. Extensive photoreceptor degeneration was subsequently observed in the adult animal. Constitutively active RAC1 formed a complex with the polarity protein PAR6 and with microtubule motor dynein in mouse retina. The normal localization of the PAR6 complex was disrupted in CA RAC1-expressing rod photoreceptors.

Conclusions. Constitutively active RAC1 had a profound negative effect on mouse rod cell viability and development. Rod photoreceptors in the CA RAC1 retina exhibited a defect in polarity and migration. Constitutively active RAC1 disrupted rod morphogenesis and gave a phenotype resembling that found in the Crumbs mutant. PAR6 and dynein are two potential downstream effectors that may be involved in CA RAC1-mediated defective mouse photoreceptor morphogenesis.

Keywords: RAC1, mouse rod morphogenesis, lamination, positioning and polarity, photoreceptor degeneration

Mammalian rod photoreceptors are highly polarized neurons that lie in the distal region of the retina, which includes the outer and inner segment (OS/IS) layer, the outer nuclear layer (ONL), and the outer plexiform layer (OPL), containing synapses. The OS is a modified primary cilium that elaborates into a stack of membranous discs that contain light-sensitive rhodopsin and components for phototransduction. The IS contains the essential biosynthetic and metabolic machinery of the cell. The functionally distinct OS and IS compartments are joined by a connecting cilium. The OS/IS points apically, while the cell sprouts an axon basally that forms a synaptic terminus in the OPL. These highly polarized morphological features are crucial for the development and function of photoreceptors.[1,2]

Photoreceptors undergo considerable morphological change from the postmitotic precursor during retinal development. After terminal mitosis, newly differentiating photoreceptors develop in polarized fashion with the IS developing first, followed by axons and the OS.[3,4] The IS starts to elaborate as the cell initiates polarity, and subsequently the OS discs bud apically from the IS. These events establish proper polarity in developing photoreceptors and are critical for OS/IS formation. The OS frequently is defective in retinal degenerative deseases.[5] Thus, understanding photoreceptor morphogenesis and plasticity may contribute insights for development of therapeutic interventions.

The two proteins, rhodopsin and peripherin/RDS, are involved in rod outer segment (ROS) formation, and rod photoreceptor cells fail to develop an OS if either of these proteins is missing.[6–10] A remarkable finding in *Drosophila* retina demonstrated that dominant active RAC1 (V12Drac1, Ras-related C3 botulinum toxin substrate 1) can mediate rhabdomere formation in rhodopsin-null photoreceptors, implicating RAC1 as a critical player in photoreceptor morphogenesis.[11] The small GTPase RAC1 is a key regulator of the actin cytoskeleton.[12,13] RAC1 responds to extracellular signals and

switches between the inactive GDP-bound and active GTP-bound forms that regulate a variety of cellular processes, including cell–cell adhesion, microtubule dynamics, cell polarity, migration, morphogenesis, and apoptosis.[14–16]

In frog, RAC1 colocalizes with rhodopsin transport carriers in photoreceptors, suggesting that RAC1 participates in the polarized trafficking into the ROS and affects photoreceptor polarity in vertebrates.[17] RAC1 is also expressed in mammalian photoreceptors,[18–21] and in mouse, activated RAC1 is involved in light-induced photoreceptor degeneration.[20,21] Hence, we explored whether constitutively active (CA) RAC1 affects mouse photoreceptor health and morphogenesis. We created transgenic mice that express CA RAC1 (similar to V12Drac1 used in the *Drosophila* study) specifically in rod photoreceptors using the mouse *Rhodopsin* promoter. The present study was conducted to characterize the phenotype of these transgenic mice and evaluate a possible effect of CA RAC1 on rod cell viability and morphogenesis.

Methods

Transgenic Mice

All animal experimental protocols were approved by the National Institutes of Health (NIH) Animal Care and Use Committee and adhered to the ARVO Statement for the Use of Animals in Ophthalmic and Vision Research. *Myc*-tagged $Rac1^{G12V}$ (constitutively active mutant, *CA Rac1*) was amplified from a cDNA clone of N-terminal *Myc*-tagged human $Rac1^{G12V}$ (Missouri S&T cDNA Resource Center, www.cdna.org). The Gly-12 to Val substitution in CA RAC1 inhibits the intrinsic GTPase-activating protein (GAP)-stimulated GTPase activity and locks RAC1 in a constitutively active GTP-bound state.[22] A *Sal*I site and a *Kozak* sequence (GCCACCATGG) were added to the 5′ end, and a *Bam*HI site and one more stop codon were added to the 3′ end of *CA Rac1*. The following primers were used during PCR amplifications: forward primer 5′-GAG AGT CGA CGC CAC CAT GGA GCA GAA GCT GAT C-3′ and reverse primer 5′-GCC TGG ATC CTT ATT ACA ACA GCA GGC ATT TTC TCT TCC-3′. The purified PCR product was cloned into a plasmid vector between a mouse *Rhodopsin* promoter and a mouse *Protamine I polyadenylation* (*PolyA*) sequence.[23] The final transgenic fragment containing *Rhodopsin promoter-CA Rac1-Protamine I PolyA* was removed from the plasmid with restriction endonucleases *Kpn*I and *Spe*I and was used for mouse (C57BL/6) pronuclear microinjections at the National Eye Institute (NEI) Genetic Engineering Core Facility. Transgenic founder mice were selected by PCR genotyping of tail genomic DNA using the following primers: forward primer 5′-CAG AGG AGG ATC TGG AGC AGA AGC-3′ and reverse primer 5′-TGT TGG GAC AGT GGT GCC GC-3′. Transgenic lines were established by crossing CA RAC1 transgenic mice with C57BL/6J mice (Jackson Laboratory, Bar Harbor, ME, USA) and maintained in a dim white fluorescence light (60 lux) room with a cycle of 12 hours dark/12 hours light. Constitutively active RAC1 transgenic and nontransgenic wild-type (WT) littermates were used in the experiments.

Western Blotting

Retinal extracts were prepared as described by Belcastro et al.[24] Equal amounts of proteins from each sample were resolved by SDS-PAGE and analyzed by Western blotting on an Odyssey Infrared Imaging System (LI-COR Biosciences, Lincoln, NE, USA). Constitutively active RAC1 and endogenous RAC1 expression were examined in mice from two transgenic lines at ages P4, P6, and P11, $n = 2$ at each time point.

Histology and Immunohistochemistry

Whole eyes were fixed overnight in 4% paraformaldehyde and 0.1% glutaraldehyde at 4°C. Fixed eye tissues were cryoprotected, embedded, and snap-frozen in Tissue-Tek O.C.T. compound (Sakura Finetek USA, Inc., Torrance, CA, USA) and cryosectioned to obtain 10-μm-thick sections. For retinal histologic analysis, cryosections were cut through the optic nerve and stained with hematoxylin and eosin (HE), visualized, and photographed using a Nikon eclipse microscope (E800; Nikon, Tokyo, Japan) with digital camera (DS-Ri1; Nikon). Mislocalized photoreceptor cells were quantified by counting nuclei along the entire length of the presumptive subretinal space in photomicrographs of HE-stained sections. Nuclei were counted in mice from two transgenic lines at ages P6 and P11 ($n = 3$ mice, three sections per mouse, at each age per transgenic line). The ONL thickness was evaluated by counting rows of ONL nuclei across the ONL width at 200-μm intervals in the region between 200 and 1000 μm from the optic nerve. Counting was done in the inferior and superior halves of the retinal sections. For each genotype, nine sections from three animals at each age (P21 and P3 months) were counted.

For immunostaining analysis, cryosections were washed in PBST (0.1% Triton X-100 in PBS) and blocked in blocking buffer (20% goat serum and 0.5% Triton X-100 in PBS) or when necessary were subjected to antigen retrieval in the Digital Decloaking Chamber (DC2002; Biocare Medical, Concord, CA) with 1× Rodent Decloaker at 95°C for 45 minutes. Then, the slides were incubated with primary antibodies (Table) overnight at 4°C, washed in PBST, and incubated with secondary antibodies, anti-rabbit Alexa Fluor 488 or 568 and anti-mouse Alexa Fluor 488 or 568 (all 1:1,000; Invitrogen, Eugene, OR, USA). Retinal nuclei were counterstained with 4′,6′-diamidino-2-phenylindole (DAPI; Invitrogen), and sections were mounted in Fluoro-Gel buffer (Electron Microscopy Sciences, Hatfield, PA) for imaging. The images were generated and analyzed by the LSM 700 confocal Microscope (Carl Zeiss Microscopy, Jena, Germany) with ZEN LE software, and further edited using Adobe Photoshop CS4, Version 11.0 (Adobe Systems, Inc., San Jose, CA, USA). Examination was done on three to four animals for each genotype per age group (P6, P11, or P24).

Terminal Deoxynucleotidyl Transferase dUTP Nick End Labeling (TUNEL) Staining

TUNEL staining was performed using the In Situ Cell Death Detection Kit (TMR red; Roche Applied Science, Mannheim, Germany) according to the manufacturer's procedure. Briefly, fixed cryosections were incubated in permeabilization solution (0.1% Triton X-100, 0.1% sodium citrate), rinsed in PBST, subsequently incubated with TUNEL reaction mixture. The sections were then counter-stained with DAPI and processed for imaging as described under Immunohistochemistry. TUNEL-positive cells were counted in the inferior and superior halves of the retinal sections from three controls and three transgenic animals at P24.

Transmission Electron Microscopy (TEM)

Eyes were fixed in 2% formaldehyde and 2% glutaraldehyde overnight at 4°C. Eye cups were postfixed in 2% osmium tetroxide, dehydrated in a graded ethanol series, and infiltrated overnight on a rotator in a 1:1 mixture of propylene oxide and Embed 812 (Electron Microscopy Sciences) prior to embedding and polymerization in freshly prepared Embed 812 at 60°C for 24 hours. One-micron sections were collected on glass slides and stained with toluidine blue to identify regions for TEM analysis. Block faces were trimmed, and pale gold thin

TABLE. List of Primary Antibodies Used in Immunohistochemistry

Name	Target	Host	Dilution	Product Source
MYC-Tag	CA RAC1	Mouse	1:2,000	2276; Cell Signaling Technology, Inc., Danvers, MA, USA
		Rabbit	1:400	2272; Cell Signaling Technology, Inc.
Cone arrestin	Cone	Rabbit	1:10,000	AB15282; Millipore, Temecula, CA, USA
Rhodopsin	Rod	Mouse	1:10,000	O 4886; Sigma-Aldrich, St. Louis, MO, USA
Retinoschisin	IS marker	Rabbit	1:1,000	Takada et al.[57]
Synaptophysin	Presynaptic marker	Mouse	1:200	S 5768; Sigma-Aldrich
PKCα	Rod bipolar cell	Rabbit	1:1,000	P 4334; Sigma-Aldrich
PH3	Mitosis marker	Rabbit	1:100	06-570; Millipore
Ki67	Progenitor cell marker	Mouse	1:400	556003; BD Biosciences, San Jose, CA, USA
BrdU	DNA synthesis marker	Rat	1:100	Ab6326; Abcam, Inc., Cambridge, MA, USA
PAR6	Polarity protein	Rabbit	1:100	Sc-67393; Santa Cruz Biotechnology, Dallas, TX, USA
PAR3	Polarity protein	Rabbit	1:50	11085-1-AP; Proteintech Group, Chicago, IL, USA
aPKCλ	Polarity protein	Rabbit	1:100	Sc-11399; Santa Cruz Biotechnology
β-catenin	OLM marker	Mouse	1:300	610153; BD Biosciences
DIC	Dynein intermediate chain	Mouse	1:400	MAB1618; Millipore

sections (90–100 nm) were collected on copper grids and stained with 2% aqueous uranyl acetate and Reynolds lead citrate. Thin sections were imaged on an electron microscope (JEM 1010; JEOL USA, Inc., Peabody, MA, USA). Transmission electron microscopy analysis was performed on multiple sections from two different animals for each genotype at P11 and P21.

BrdU Pulse-Chase Assay

Mice were injected intraperitoneally at P1 with BrdU (100 μg/g; Sigma-Aldrich, St. Louis, MO). Eyes were collected at 3 hours (P1), 4 days (P5), and 10 days (P11) after injection, fixed in 4% paraformaldehyde overnight at 4°C, and cryosections were obtained. The samples were pretreated with 2N HCl at 37°C for 50 min, neutralized by 0.1 M borate buffer, blocked in blocking buffer and then subjected to double immunostaining with anti-BrdU and anti–rhodopsin antibodies. For each genotype, BrdU assay was done on at least three animals at each time point.

Immunoprecipitation (IP)

Retinal extracts prepared in IP buffer consisting of 10 mM Tris-HCl (pH 7.4), 5 mM EDTA, 20% glycerol, and Halt protease inhibitor cocktail (Thermo Fisher Scientific, Inc., Pierce Biotechnology, Rockford, IL, USA) were precleared by incubation with protein G-agarose beads (Invitrogen, Carlsbad, CA, USA) for 1 hour at 4°C. Precleared extracts were incubated with the following antibodies overnight at 4°C according to the manufacturer's instructions: Anti-RAC1, clone 23A8, agarose conjugate (Millipore, Temecula, CA, USA), or MYC-Tag mouse mAb (sepharose bead conjugate; Cell Signaling Technology, Danvers, MA, USA) or mouse IgG (sepharose bead conjugate; Cell Signaling Technology). The beads were separated from the supernatant by centrifugation and washed three times with IP buffer. To elute bound immunocomplexes, the beads were resuspended in Laemmli buffer and heated to 100°C for 5 minutes. Bound immunocomplexes were detected by Western blot on an Odyssey Infrared Imaging System (LI-COR Biosciences) using antibodies against RAC1 (mouse, 1:1000; Millipore), PAR6 (rabbit, 1:200; Santa Cruz Biotechnology, Dallas, TX, USA), DIC (dynein intermediate chains, mouse,1:1000; Millipore), and KHC (kinesin heavy chain, mouse, 1:500; Millipore). The results shown are from one of three different experiments on transgenic and control animals at P11 that yielded similar results.

Electroretinography (ERG)

Full-field (Ganzfeld) scotopic ERGs were recorded from CA RAC1 transgenic and nontransgenic control littermates at P21 following the procedures described previously.[25] Briefly, mice were dark adapted overnight before anesthesia with intraperitoneal ketamine (70 mg/kg) and xylazine (6 mg/kg), and pupils were dilated with 0.5% tropicamide and 0.5% phenylephrine HCl. Dark-adapted ERG responses were elicited using single flashes from a xenon discharge source (Grass Photic Stimulator PS33; Astro-Med, Inc., West Warwick, RI) from −6.9 to +0.6 log cd-s/m^2 at 0.5 log unit intervals. All procedures were performed under dim red light. A-waves were measured from the prestimulus baseline to the initial trough at intensities from −2.4 to +0.6 log cd-s/m^2. Rod b-waves were measured from the baseline or from the a-wave trough when present to the peak at intensities from −4.9 to −1.4 log cd-s/m^2. Measurements were made on five to six animals for each genotype.

Statistical Analysis

Quantitative data are presented as mean ± SEM. Student's *t*-test was used to compare the average number of mislocalized cell nuclei in the presumptive subretinal space and the number of ONL nuclei in CA RAC1 transgenic lines at different ages. Statistical comparison of a-wave and b-wave amplitudes was done across a range stimulus intensities using the *t*-test and correcting for multiple comparisons using the Holm-Sidak method in GraphPad Prism 6.01 for Windows (GraphPad Software, La Jolla, CA, USA).

RESULTS

Disrupted Laminar Morphology and Photoreceptor Localization in CA RAC1 Retinas

Constitutively active RAC1 expression under control of the *Rhodopsin* promoter could be detected by postnatal day (P)4 with Western blotting in the transgenic mice, and by P6, it reached 19% and 41% of endogenous RAC1 level in two transgenic lines, designated LO and HI lines, respectively (Figs. 1A, 1B).

Both CA RAC1 LO and HI lines displayed a similar phenotype but to a variable degree that was consistent with the level of CA RAC1 expression. Morphological features of the phenotype in both lines are shown in Figure 2A, but in

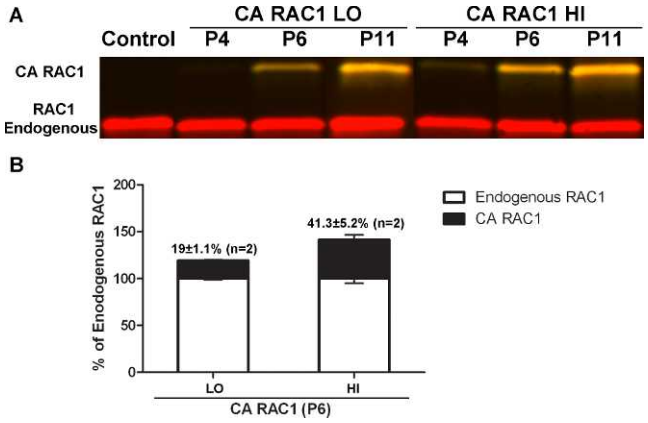

FIGURE 1. Constitutively active RAC1 expression in transgenic mice. (**A**) Western blotting with anti-RAC1 (endogenous RAC1 and transgenic CA RAC1) and anti-MYC-Tag (transgenic CA RAC1-specific) antibodies at P4, P6, and P11 indicated that CA RAC1 expression in the retinas increased with age in both LO and HI transgenic lines. Constitutively active RAC1 protein bands are yellow due to an overlap of anti-RAC1 (*red*) and anti-MYC-Tag (*green*) antibodies. (**B**) Fluorescence values of the CA RAC1 band in each sample at P6 were normalized to fluorescence values of corresponding endogenous RAC1 band. Quantification of CA RAC1 expression is represented as a percentage of endogenous RAC1 levels in CA RAC1 retinas, shown by the bar graph (mean ± SEM, $n = 2$).

subsequent figures, we show the results for only the LO line. At P4, morphology of the CA RAC1 retina was indistinguishable from the WT control (Figs. 2Aa–c). However, by P6, some photoreceptor cell nuclei were observed in the presumptive subretinal space adjacent to the retinal pigment epithelium (RPE) in both transgenic lines (Figs. 2Ae, 2Af; Figs. 3Ac–e). The ONL in the HI-expressing line (Fig. 2Af) had far fewer nuclei and was approximately half as thick as littermate controls (Fig. 2Ad) at P6. The morphological and positioning defects became more extensive by P11 and caused folds and whorls of the ONL in the central retinal region (Figs. 2Ah, 2Ai). More nuclei were mislocalized to the presumptive subretinal space by P11 than at P6 (Fig. 2Ah versus Fig. 2Ae, Fig. 2Ai versus Fig. 2Af; LO line, 755 ± 44 at P11 vs. 105 ± 23 at P6, $n = 3$, $P < 0.001$; HI line, 1086 ± 97 at P11 vs. 301 ± 84 at P6, $n = 3$, $P < 0.01$). Lamination of the OPL that contains the photoreceptor synaptic termini was also distorted and gave incomplete separation of the ONL from the inner nuclear layer (INL). The INL in transgenic retinas contained a large number of rhodopsin-labeled rods expressing transgenic CA RAC1 (Figs. 3Ad, 3Ai). These mislocalized rods were found as early as P6 and remained there at P11. The developmental course of abnormal ONL lamination in the CA RAC1 retina, along with early mislocalization of rods to the INL, indicates that CA RAC1 interrupts normal positioning and lamination of developing rod cells.

By P21, the CA RAC1 HI line had significantly fewer ONL nuclei (four to six rows thick) than the LO line with five to eight rows ($P < 0.0001$, $n = 3$) (Figs. 2Ak, 2Al). The WT littermate controls had 10 to 11 rows ($n = 3$) in the ONL at this age (Fig. 2Aj). The a- and b-wave amplitudes of the dark-adapted ERG in P21 CA RAC1 LO mice ($n = 5$) were both diminished to 54% ($P < 0.0001$ and $P < 0.01$, respectively) of the controls ($n = 6$) at their respective maximum stimulus intensities (see Methods). Thus, the decrease in ONL cell numbers alone accounted for most of the reduction in a- and b-wave amplitudes. By 3 months of age, the ONL was reduced to a single row of nuclei in the HI line and two to three rows in the LO line, and retinal folds or whorls were no longer seen

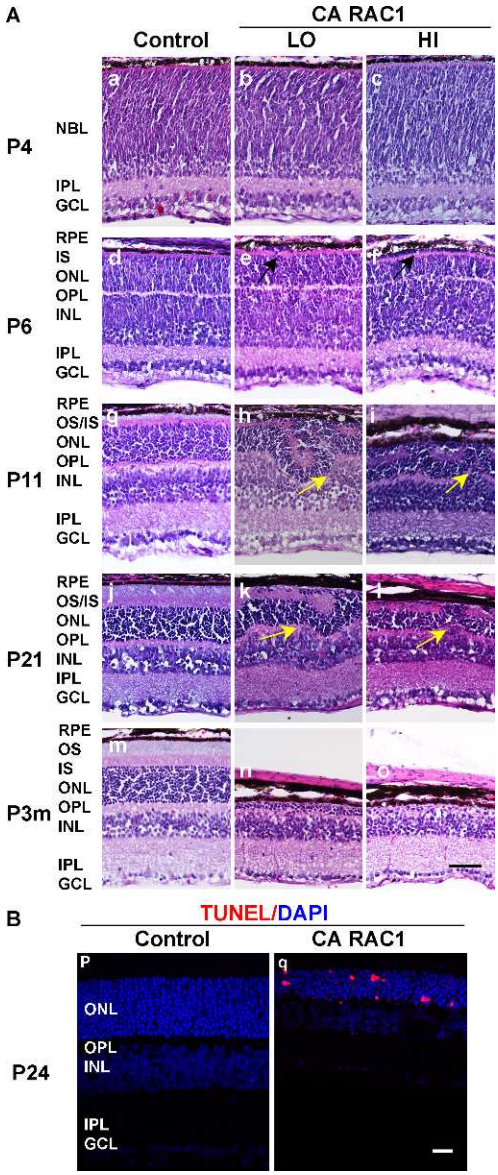

FIGURE 2. Time course of abnormal outer nuclear layer (ONL) lamination in CA RAC1 retinas during retinal development. (**A**) Retinal sections from CA RAC1 (LO and HI) and nontransgenic WT (Control) littermates at several postnatal times (P4, P6, P11, P21, and P3m) stained with hematoxylin and eosin showed progressive defects in the ONL lamination of CA RAC1 retinas. At P4, CA RAC1 retinas (**b**, **c**) had apparently normal neuroblastic layers (NBL). At P6, the IS appeared in both control (**d**) and CA RAC1 (**e**, **f**) retinas, but some nuclei were mislocalized into the space between the RPE and IS layer in CA RAC1 retinas (**e**, **f**) (*black arrows*). The OPL formed closer to the apical margin of the ONL than in the control, leading to a thin ONL, particularly in the CA RAC1 HI line (**f**). At P11, additional nuclei were displaced into the presumptive subretinal space adjacent to the RPE in both transgenic lines (**h**, **i**). ONL nuclei aberrantly formed retinal folds or whorls in the central retinal region. *Yellow arrows* indicate the areas bridging ONL to INL with incomplete separation by the OPL. By P21, both LO and HI lines had fewer ONL nuclei (**k**, **l**), compared with the WT control (**j**). By 3 months (P3m), the ONL was reduced to a single layer of nuclei in the HI line (**o**) and two to three rows in the LO line (**n**). *Scale bar*: 50 μm. (**B**) Retinal sections of nontransgenic control (Control) and CA RAC1 littermates at P24 with TUNEL assay showed increased apoptosis signals (*red*) at ONL in CA RAC1 retinas (**q**), compared to the control (**p**). *Scale bar*: 20 μm. IPL, inner plexiform layer, GCL, ganglion cell layer.

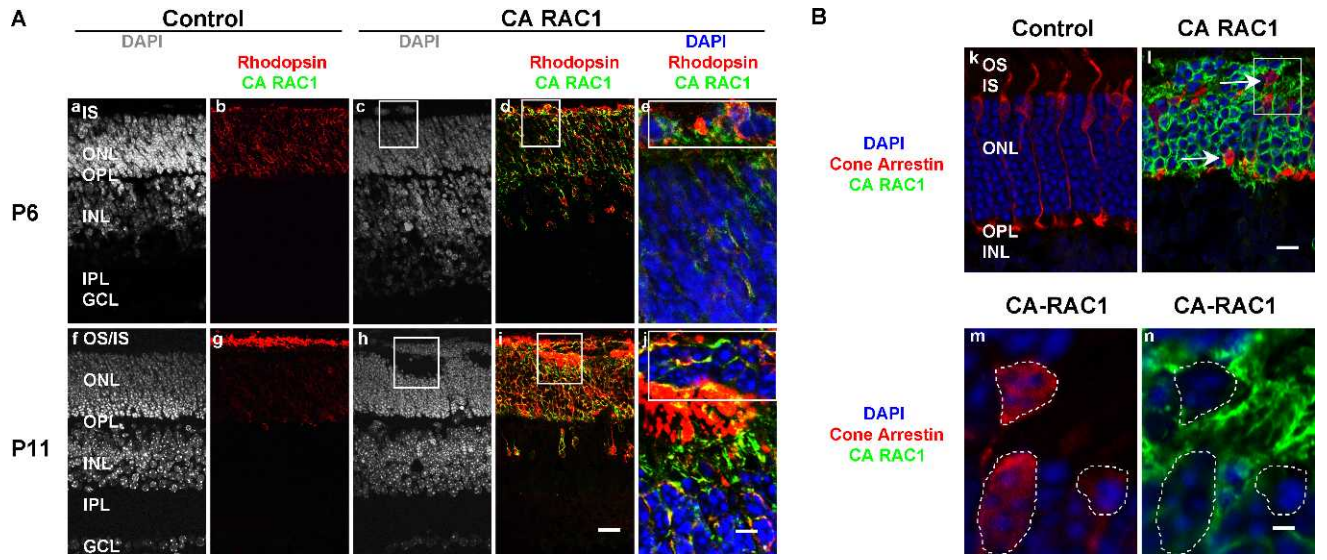

Figure 3. Mislocalization of rod and cone photoreceptors in CA RAC1 retinas. Retinal sections of nontransgenic control and CA RAC1 mice were double immunostained with antibodies against MYC-Tag (*green*, CA RAC1) and rhodopsin (*red*) (**A**) or cone arrestin (*red*) (**B**). Retinal nuclei were labeled with DAPI (*gray* or *blue*). (**A**) Representative DAPI and merged images are shown. Mislocalized cells in the subretinal space in CA RAC1 retinas at P6 ([**c**–**e**], *boxed regions*) and at P11 ([**h**–**j**], *boxed regions*) were positive for CA RAC1 (*green*) and rhodopsin (*red*) double immunostaining (higher magnification images of boxed regions in [**d**] and [**i**] are shown in [**e**] and [**j**], respectively), indicating that these mislocalized cells were rod photoreceptors. Many more cells double-labeled with CA RAC1 (*green*) and rhodopsin (*red*) antibodies were mislocalized in the INL at P6 (**d**) and P11 (**i**), compared to the control (**b**, **g**). (**a**–**d**, **f**–**i**) *Scale bar*: 20 μm; (**e**, **j**) *scale bar*: 5 μm. (**B**) Merged immunostaining images of CA RAC1 (*green*) and cone arrestin (*red*) are shown in the control (**k**) and CA RAC1 (**l**) retinas at P24. Cone arrestin–positive somas were located at the apical surface of the ONL in the control, whereas cone arrestin–stained cell bodies were mislocalized in the CA RAC1 retina ([**l**], *white arrows*). (**k**, **l**) *Scale bar*: 10 μm. A magnified region of the white box in (**l**) is shown in (**m**, **n**). *Dotted outlines* in (**m**, **n**) display the location of cone arrestin–positive cell bodies, indicating that the cone cells were negative for CA RAC1 staining in CA RAC1 retinas. *Scale bar*: 2.5 μm.

(Figs. 2An, 2Ao). We examined retinas by TUNEL assay at P24 and found that CA RAC1 retinas had a greater number of apoptotic cells in the ONL (19 ± 3, $n = 3$) compared with control retinas which had nearly no TUNEL-positive cells in any layer (Fig. 2B), implicating apoptosis in ONL cell loss.

The CA RAC1 protein was expressed in rods but not cones (identified using cone arrestin labeling, Fig. 3B) or Müller cells (not shown). Cone nuclei normally reach their final position at the apical side of the ONL by P12[26] (Fig. 3Bk). However, in CA RAC1 retinas even at P24, cone arrestin–positive cone soma remained distributed throughout the ONL, and some were mislocalized to the subretinal space adjacent to the RPE (Fig. 3Bl). Double labeling with the MYC-Tag antibody showed that these cones did not express the CA RAC1 protein (Figs. 3Bm, 3Bn), implying that the mislocalization of cone nuclei is an indirect effect of CA RAC1 expression.

Abnormal Polarity of the Ectopic Photoreceptors Adjacent to the RPE

Disrupted retinal lamination has been associated with cell polarity defects.[27–31] To evaluate the polarity of the mislocalized rod photoreceptors in the CA RAC1 retina, we looked at IS/OS formation using antibodies against retinoschisin, which localizes to IS, and rhodopsin (for OS). Although the plasma membrane of these ectopic rods adjacent to the RPE stained for rhodopsin at P11 and P21, none showed IS/OS labeling protruding toward the RPE, indicating that normal orientation was disrupted (Figs. 4Ab, 4Ad). Transmission electron microscopy ultrastructure at P11 (not shown) and at P21 also showed no normally polarized IS/OS structures associated with the ectopic mislocalized soma (Fig. 4Bf). These results indicate that mislocalized rods adjacent to the RPE fail to elaborate the normal IS/OS in the CA RAC1 retina.

Further polarity miscues were evident in the aberrant placement of synapses of the ectopic rods, shown by double immunolabeling using synaptophysin as a presynaptic marker and protein kinase C alpha (PKCα) to mark rod bipolar cells and processes. These aberrant synapses had no contact onto rod bipolar cells (Fig. 4C). Transmission electron microscopy showed a free floating synaptic ribbon in an ectopic photoreceptor in the subretinal space (Figs. 4Dj, 4Dk). The displaced synaptic ribbon was surrounded by apparently normal vesicles, although the ribbon projected toward the RPE, and no postsynaptic elements were observed at the site. The failure to elaborate normal IS/OS along with failure of synaptic localization indicates that the ectopic rod cells lacked proper polarity.

Improper Migration of Differentiating Rod Photoreceptors

Rod cell nuclei were mislocalized into the subretinal space as early as P6 (Fig. 2A) when some retinal cells normally are still in a proliferation stage.[32] The number of mislocalized cells increased by P11 (Fig. 2A). However, no retinal progenitor cells (RPCs) were found among these mislocalized cells using antibodies against phospho-histone H3 (pH3, specific for mitotic RPCs) and Ki67 (labels RPCs in all active phases of the cell cycle) (Figs. 5Ae, 5Ag). The distribution of pH3 and Ki67 signals was similar in CA RAC1 and control retinas at P6 (Fig. 5A). Thus, the localization of RPCs is not affected in the CA RAC1 retina.

Using BrdU pulse administered by intraperitoneal injection at P1 to label DNA synthesis (S)-phase RPCs, we tracked the

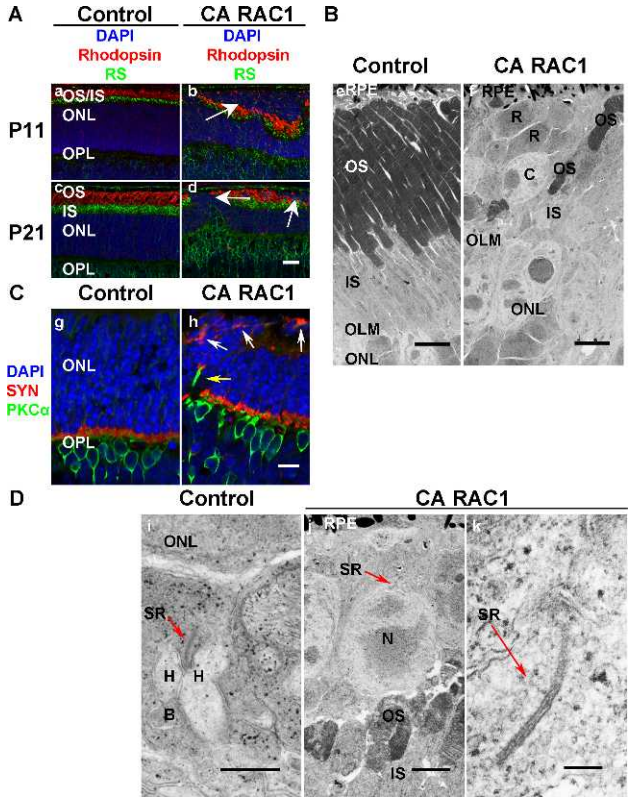

Figure 4. Characterization of mislocalized rod cells in the presumptive subretinal space adjacent to the RPE in CA RAC1 retinas. (**A**) Rod photoreceptor IS and OS were immunostained with antibodies against retinoschisin (RS, *green*) and rhodopsin (*red*), respectively, at P11 and P21. In the CA RAC1 retina (**b**, **d**), the mislocalized photoreceptors in the subretinal space (*white arrows*) did not show any normally oriented RS (*green*) and rhodopsin (*red*) labeling. *Scale bar*: 20 μm. (**B**) TEMs of photoreceptor cells are shown for nontransgenic control (**e**) and CA RAC1 (**f**) retinas at P21. No IS/OS structure was found between mislocalized cells (R, C) and the RPE (**f**). Note that mislocalized cells adjacent to the RPE included rods (R, large clumps of heterochromatin typical of rod nuclei) and cones (C, one or more small clumps of heterochromatin surrounded by a large amount of lighter staining euchromatin characteristic of cone nuclei). *Scale bars*: 5 μm. (**C**) Photoreceptor synaptic terminals were detected by immunostaining with synaptophysin (SYN, *red*), a presynaptic marker, and protein kinase C alpha (PKCα, *green*), a rod bipolar cell marker. In comparison to the nontransgenic control (**g**) in which a continuous band of staining with SYN and PKCα was seen across OPL synaptic terminals, the CA RAC1 retina showed a fragmented staining pattern (**h**). In the CA RAC1 retina, ectopic staining of SYN was observed around apically mislocalized cells that was not associated with PKCα-stained rod bipolar cells ([**h**], *white arrows*) and PKCα-positive bipolar cell process protruded into the ONL to contact synaptic terminals ([**h**], *yellow arrow*). *Scale bar*: 10 μm. (**D**) TEM images of synaptic ribbons (SR) are shown in the nontransgenic control ([**i**], *red arrow*) and in a mislocalized cell adjacent to the RPE in the CA RAC1 retina ([**j**], *red arrow*). A higher magnification image of SR in (**j**) is shown in (**k**) (*red arrow*). Note that, in the CA RAC1 retina, a displaced ribbon tethered multiple vesicles and pointed toward the RPE. No horizontal (H) or bipolar (B) cells were found around the ribbon. N, nucleus. (**i**) *Scale bar*: 500 nm; (**j**) *scale bar*: 2 μm; (**k**) *scale bar*: 100 nm.

newly born cells in the retina at P1, P5, and P11 (Fig. 5B). Three hours after BrdU was injected, the distribution of labeled RPCs was similar in CA RAC1 and control retinas and was confined primarily to the middle of the neuroblastic layer. By P5, BrdU-positive cells were distributed throughout the ONL and INL in both CA RAC1 and control retinas. However, a few BrdU-labeled cells in the CA RAC1 retina were already mislocalized to the subretinal space (Fig. 5Bm, arrows), and by P11, additional BrdU-labeled cells had migrated to the subretinal space (Fig. 5Bn, arrows). Double labeling with anti-BrdU and rhodopsin antibodies confirmed that these were differentiated rod photoreceptors (Fig. 5B, inset in o). These results indicate that the mislocalized photoreceptors reached the subretinal space due to improper migration of differentiating rods. Defective migration may be due to a direct effect of CA RAC1 expression in the mislocalized rod cells and/or an indirect effect, e.g., via disruption of the outer limiting membrane (OLM). The BrdU experiment does not distinguish between these two possibilities.

Interrupted Localization of the PAR6 Complex, a Protein Partner of CA RAC1, in the CA RAC1 Retina

We explored possible molecular mechanisms for the abnormal positioning and cell polarity signals by identifying potential protein partners of CA RAC1. The polarity PAR6 (partition-defective 6) complex consists of PAR3, PAR6, and atypical PKCλ (aPKCλ) and has been implicated in retinal lamination in mouse[30] and is required for photoreceptor morphogenesis and polarity in *Drosophila*.[33] Although RAC1-GTP can bind to the PAR6 in epithelial cells,[34,35] thereby providing a possible link between RAC1 activation and PAR6 complex–cell polarity signaling, interaction of RAC1 with PAR6 has not been reported for the mammalian retina. Immunoprecipitation with RAC1 antibody pulled down PAR6 along with endogenous RAC1 and CA RAC1 from CA RAC1 retinal extracts (Fig. 6A, CA RAC1, RAC1-IP). We also found that PAR6 was pulled down with endogenous RAC1 from WT control retinal extracts (Fig. 6A, Control, RAC1-IP). The MYC-Tag antibody, which is specific for CA RAC1, also co-immunoprecipitated (co-IP) PAR6 along with CA RAC1 (Fig. 6A, CA RAC1, MYC-IP). Double immunolabeling with MYC-Tag and PAR6 antibodies showed colocalization of CA RAC1 with PAR6 in situ (Fig. 6B). Together with the co-IP results, these demonstrate that CA RAC1 and PAR6 can form a complex in the murine retina.

Since apical localization of the PAR6 complex is essential for establishing proper cell polarity,[33,36–41] we examined the distribution in the CA RAC1 retina. In contrast to a continuous labeling pattern for three components of the PAR6 complex (PAR6, PAR3, and aPKCλ) in WT controls, labeling in the CA RAC1 retina was interrupted by the ectopic mislocalized photoreceptor cells adjacent to the RPE (Fig. 6C). This suggests that CA RAC1 may disrupt photoreceptor polarity by interrupting the asymmetric localization of the PAR6 complex at the apical side of the ONL. Fragmented staining of β-catenin (an OLM marker) (Fig. 6C) indicated that the OLM integrity was impaired in the CA RAC1 retina and may contribute to defective ONL lamination.

CA RAC1 Complexes With Dynein in the Retina

The rods with nuclei in the INL showed morphologies with long trailing processes extending apically toward the ONL (Fig. 7A), suggesting that the nucleus, but not the entire cell, is displaced into the INL. Studies in *Drosophila* and zebrafish have indicated a critical role for minus-end (dynein/dynactin) and plus-end (kinesin) directed microtubule motors in photoreceptor nuclear migration and positioning.[42,43] We evaluated whether CA RAC1 might regulate nuclear positioning of mouse photoreceptors by interacting with dynein and kinesin. Following IP with RAC1 antibody from CA RAC1 retinal extracts, the associated dynein intermediate chain (DIC) was detected in the co-IP complex by Western blotting, but specific binding of kinesin heavy chain (KHC) was not detected (Fig. 7B, RAC1-IP). Immunoprecipitation of CA

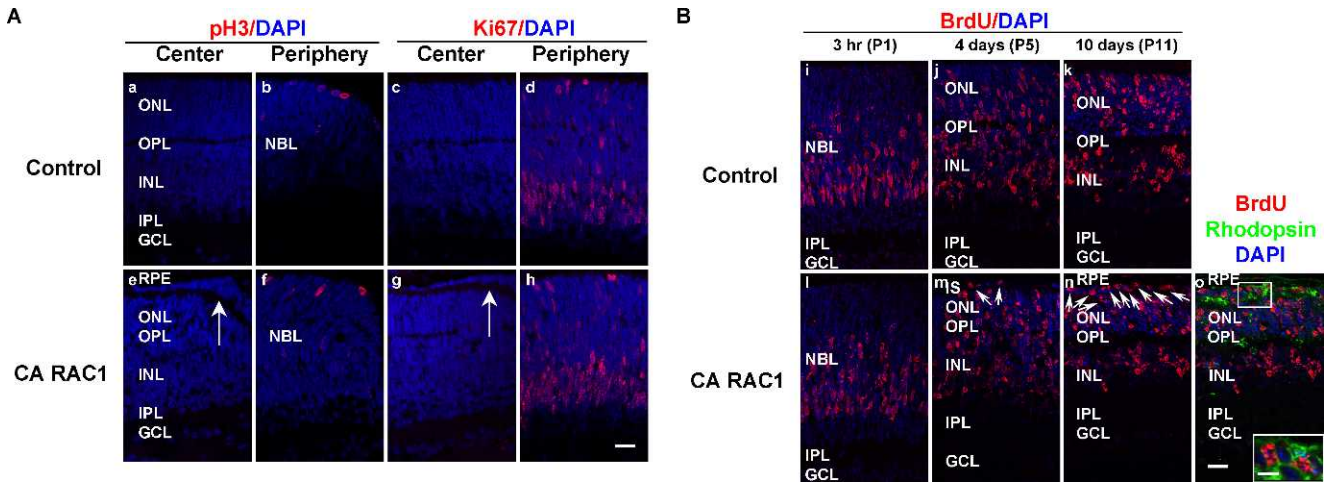

Figure 5. Localization of retinal progenitor cells and migration of newly differentiated photoreceptors in CA RAC1 retinas. (**A**) Retinal sections of CA RAC1 and nontransgenic littermates (Control) at P6 immunostained with the antibody against pH3 (*red*, [**a**, **b**, **e**, **f**]) or Ki-67 (*red*, [**c**, **d**, **g**, **h**]). Nuclei were counterstained with DAPI. Images of central and periphery regions show similar staining patterns of pH3 and Ki-67 in control (**a**–**d**) and CA RAC1 (**e**–**h**) retinas. Note that no pH3- or Ki-67-positive labeling was detected within the mislocalized nuclei adjacent to the RPE ([**e**] and [**g**], *white arrows*). (**B**) The movement of BrdU-labeled cells in CA RAC1 retinas. Immunofluorescence images of BrdU-labeled cells (*red*) in nontransgenic control (**i**–**k**) and CA RAC1 (**l**–**n**) retinas are shown at 3 hours (P1), 4 days (P5), and 10 days (P11) after BrdU injection at P1. In CA RAC1 retinas, more mislocalized cells in the subretinal space (indicated by *white arrows* in [**m**] and [**n**]) were labeled by BrdU (*red*) at P11 (**n**) than at P5 (**m**). (**o**) Double staining of BrdU (*red*, stains the nucleus) and rhodopsin (*green*, stains the plasma membrane) indicates that BrdU-positive mislocalized cells in the subretinal space also stained for rhodopsin. The inset in (**o**) is higher magnification of the *white box region*. (**i**–**o**) *Scale bar*: 20 μm. *Scale bar* in the inset: 5 μm.

RAC1 with MYC-Tag antibody also pulled down DIC, not KHC, along with CA RAC1 (Fig. 7B, MYC-IP). Immunostaining revealed that CA RAC1 colocalized with DIC in the retina (Fig. 7C). These results indicate that CA RAC1 was in a complex with dynein in the retina.

Discussion

This study demonstrates that transgenic expression of constitutively active RAC1 has a profound negative effect on developing rods and interferes with rod morphology and proper retinal lamination. The same *Rhodopsin* promoter was used previously to generate transgenic mice expressing phosducin or phosducin phosphorylation mutant and both mouse lines had normal retinal morphology.[24] Therefore, abnormal photoreceptor morphology observed in our transgenic retinas most likely resulted from CA RAC1 expression in rods rather than from a nonspecific effect of expressing the transgene from this promoter. It also appears unlikely that disrupted CA RAC1 retinal morphology is a generic and nonspecific effect limited to actin cytoskeleton regulation by RAC1 for several reasons. First, pharmacological interference of the actin network is reported to disrupt the generation of new OS discs in photoreceptors,[44] a phenotype different from what we observed in the CA RAC1 retina. Second, disruption of the actin cytoskeleton would be expected to cause defects in all CA RAC1-expressing rods, whereas in our transgenic mice, only some of the CA RAC1-expressing rods exhibited morphological defects.

Constitutively active RAC1 formed a complex with PAR6 that potentially could affect rod polarity and positioning during morphogenesis. Establishing and maintaining proper polarity and OLM integrity are factors crucial for photoreceptor morphogenesis.[29–31,33,45–47] In mammals, the classical epithelial polarity PAR6 complex (PAR3/PAR6/aPKCλ) localizes to the tight junctions in epithelial cells and to the adherens junctions (AJs) in neuroblasts, and it is a central player in the formation of the junctions and polarization in these cell types.[34,39,41,48,49] A recent study in *Drosophila* photoreceptors demonstrates that PAR6 and aPKCλ form a protein complex that colocalizes to the rhabdomere stalk (equivalent to the IS in mammalian photoreceptors) and that PAR3 localizes to the AJs.[33] All three proteins are required for the organization and maintenance of apicobasal polarity and AJs of *Drosophila* photoreceptors. Conditional deletion of aPKCλ in mouse postmitotic photoreceptors results in mislocalization of PAR3 and PAR6 and leads to defective retinal lamination and loss of photoreceptor cell polarity.[30] The normal apical localization of the PAR6 complex was disrupted in CA RAC1 retinas, suggesting that RAC1 may play an important role in recruiting the PAR6 complex to the proper location, which is essential for the complex to function in establishing cell polarity. As a result, CA RAC1 expression may interfere with the proper polarization and laminar positioning of mouse photoreceptors through interaction with PAR6.

The fragmented OLM and abnormal lamination of photoreceptors in the CA RAC1 retina resembles the phenotype observed in mouse Crumbs (CRB) mutants.[46,50] Crumbs is a conserved epithelial polarity protein, and mutations in CRB have been shown to cause a form of Leber congenital amaurosis and a form of retinitis pigmentosa, RP12, in humans.[51] A recent study indicates that RAC1 signaling mediates CRB function in *Drosophila* epithelial integrity, and constitutively active RAC1 restricts membrane localization of CRB and interferes with CRB-dependent epithelial morphogenesis.[52] This suggests the possibility that RAC1 may play a role in the regulation of CRB in humans.

Not all of the CA RAC1-expressing rod cells exhibited polarity and positioning defects, and many were in normal position and had normal IS/OS orientation (Fig. 4A) and synaptic connectivity as demonstrated by eliciting ERG responses. One likely explanation is that defects are only caused in rod cells that are expressing CA RAC1 at the time that polarity is being established but not once polarity has been established. Supporting evidence comes from other studies in which overexpression of dominant negative PAR6 or aPKCλ-kn

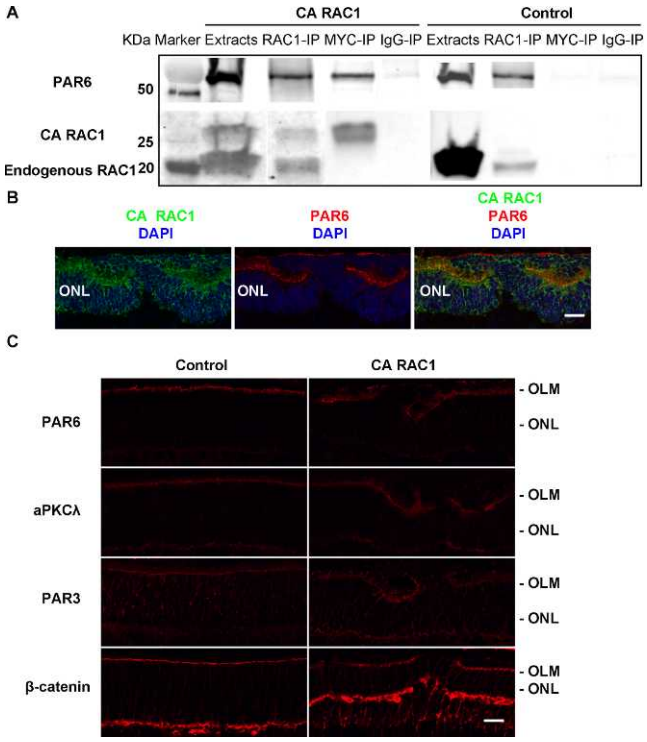

Figure 6. Disrupted localization of the PAR6 complex in the CA RAC1 retina. (**A**) Retinal extracts (Extracts) of CA RAC1 and nontransgenic WT (Control) littermates at P11 were immunoprecipitated using either anti-RAC1 (endogenous RAC1 and transgenic CA RAC1, RAC1-IP) or anti-MYC-Tag (transgenic CA RAC1-specific, MYC-IP) antibody and control IgG (IgG-IP). Co-immunoprecipitated proteins were analyzed by Western blotting. PAR6 was co-IP in both RAC1-IP and MYC-IP immunocomplexes of CA RAC1 retinal extracts, but only in RAC1-IP immunocomplex of the control. (**B**) Retinal sections of CA RAC1 mice at P11 were double immunostained with antibodies against MYC-Tag (*green*, CA RAC1) and PAR6 (*red*). Nuclei were labeled with DAPI (*blue*). Merged images indicate that CA RAC1 colocalized with PAR6. *Scale bar*: 20 μm. (**C**) Retinal sections of nontransgenic control and CA RAC1 littermates at P11 were immunostained with antibodies against components of the PAR6 complex (PAR6, aPKCλ, and PAR3) and β-catenin, an OLM marker. Immunostaining pattern of these proteins was disrupted and fragmented in CA RAC1 retinas. *Scale bar*: 20 μm.

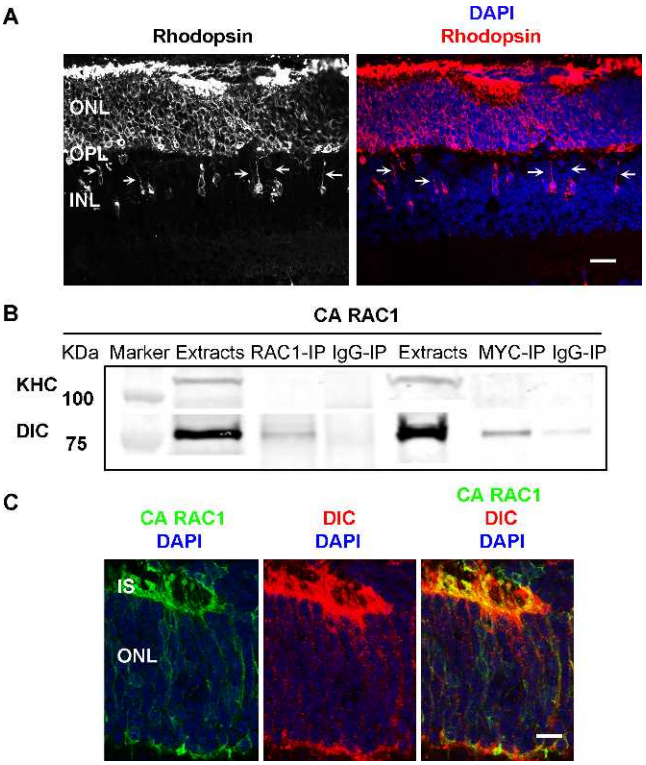

Figure 7. Constitutively active RAC1 forms a complex with dynein in the CA RAC1 retina. (**A**) Retinal sections of CA RAC1 mice at P11 were immunostained with anti-rhodopsin antibody (*gray* or *red*). Nuclei were labeled with DAPI (*blue*). Rhodopsin-stained and merged images are shown. Mislocalized cells with nuclei in the INL extended long processes toward the ONL (indicated by arrows). *Scale bar*: 20 μm. (**B**) Retinal extracts (Extracts) of CA RAC1 mice at P11 were immunoprecipitated using either anti-RAC1 (RAC1-IP) or anti-MYC-tag (MYC-IP) antibody and control IgG (IgG-IP). Dynein intermediate chain (DIC), not kinesin heavy chain (KHC), was detected in both RAC1-IP and MYC-IP immunocomplexes by Western blotting. (**C**) Retinal sections of CA RAC1 mice at P11 were double immunostained with antibodies against MYC-Tag (*green*, CA RAC1) and DIC (*red*). Individual and merged images are shown, indicating that CA RAC1 colocalized with DIC. *Scale bar*: 10 μm.

mutants in mammalian epithelial cells caused polarity defects only in cells developing polarity but not in cells already polarized.[39,53] Many of the rod photoreceptors in the CA RAC1 retina have established polarity before the *rhodopsin* promoter switches on and results in aberrant CA RAC1 signaling (Fig. 2A, P4). One possible conclusion is that CA RAC1 expression disrupts the signaling involved in establishing, rather than maintaining, proper polarization in rod cells.

Previous studies reported that normally by P5 approximately 40% of the rod nuclei lie within the INL at the time the OPL forms, and that by P8 the majority of these nuclei have migrated into the ONL.[54] Many more rod nuclei remained in the INL in the CA RAC1 retina at P6 and P11, compared to the control (Fig. 3A). Our results imply that CA RAC1 disrupted directional or timely nuclear migration of rod cells during postnatal retinal development (Fig. 7A). The mislocalization of rod nuclei into the INL (i.e., basal relative to ONL) in CA RAC1 retinas is similar to photoreceptor nuclear positioning defects observed in *Drosophila* and zebrafish retinas when the function of dynein/dynactin is disturbed.[42,43] The dynein/dynactin motor complex pulls the nucleus toward the apical side of the cell, while the kinesin motor acts in opposition to dynein/dynactin. For example, mutations in *Dynactin 1* (p150, a subunit of dynactin complex) and *Lis1* (a dynein-associated protein) cause mispositioning of photoreceptor nuclei to more basal location in flies and zebrafish. Loss of function mutations in kinesin heavy chain suppress this nuclear positioning phenotype in *Drosophila Dynactin 1* mutants.[42] Thus, positioning of photoreceptor nuclei would be governed by the relative balance between these two opposing motor activities. We found that CA RAC1 formed a complex with dynein rather than with kinesin (Figs. 7B, 7C). As a force balance controlled by dynein/dynactin and kinesin motor complexes is essential for normal nuclear migration and positioning, we can speculate that CA RAC1 may disrupt the balance by disproportionately interacting with dynein, leading to defective nuclear migration and mispositioning of photoreceptors.

Abnormal localization, however, cannot explain the increased apoptosis throughout the ONL (Fig. 2B) that leads to extensive cell loss in adult CA RAC1 retinas by 3 months of age. Active RAC1 is known to be a critical component for the activation of NADPH oxidase, which is a source of reactive oxygen species and contributes to cardiac hypertrophy[55] and neurodegeneration.[56] In addition, RAC1 activation of NADPH

oxidase has recently been linked to light-induced photoreceptor degeneration.[21] Thus, the extensive photoreceptor degeneration we observed in adult CA RAC1 retinas may result from oxidative damage through CA RAC1 acting as a component of NADPH oxidase.

These results show that constitutive activation of RAC1 in newly differentiating rods disrupted normal apicobasal and axon-dendrite polarity and positioning of rods. Many neurons, including photoreceptors, orient their axonodendritic axis corresponding to the apicobasal axis of their origin—the neuroepithelium. Our study implicates an important role for RAC1 in the process of initial polarization and morphogenesis during rod photoreceptor development.

Acknowledgments

Maria Santos and Jinbo Li provided technical assistance, and Eric Wawrousek and Steve Lee (NEI Genetic Engineering Facility) assisted in the generation of transgenic mice.

Supported by the National Institutes of Health Intramural Research Programs of the National Institute on Deafness and Other Communication Disorders and the National Eye Institute. The authors alone are responsible for the content and writing of the paper.

Disclosure: **H. Song**, None; **R.A. Bush**, None; **C. Vijayasarathy**, None; **R.N. Fariss**, None; **S. Kjellstrom**, None; **P.A. Sieving**, None

References

1. Kennedy B, Malicki J. What drives cell morphogenesis: a look inside the vertebrate photoreceptor. *Dev Dyn*. 2009;238:2115–2138.
2. Randlett O, Norden C, Harris WA. The vertebrate retina: a model for neuronal polarization in vivo. *Dev Neurobiol*. 2011;71:567–583.
3. Hinds JW, Hinds PL. Differentiation of photoreceptors and horizontal cells in the embryonic mouse retina: an electron microscopic, serial section analysis. *J Comp Neurol*. 1979;187:495–511.
4. Schmitt EA, Dowling JE. Early retinal development in the zebrafish, *Danio rerio*: light and electron microscopic analyses. *J Comp Neurol*. 1999;404:515–536.
5. Travis GH. Mechanisms of cell death in the inherited retinal degenerations. *Am J Hum Genet*. 1998;62:503–508.
6. Humphries MM, Rancourt D, Farrar GJ, et al. Retinopathy induced in mice by targeted disruption of the rhodopsin gene. *Nat Genet*. 1997;15:216–219.
7. Travis GH, Brennan MB, Danielson PE, Kozak CA, Sutcliffe JG. Identification of a photoreceptor-specific mRNA encoded by the gene responsible for retinal degeneration slow (*rds*). *Nature*. 1989;338:70–73.
8. Connell G, Bascom R, Molday L, et al. Photoreceptor peripherin is the normal product of the gene responsible for retinal degeneration in the *rds* mouse. *Proc Natl Acad Sci U S A*. 1991;88:723–726.
9. Sanyal S, Jansen HG. Absence of receptor outer segments in the retina of *rds* mutant mice. *Neurosci Lett*. 1981;21:23–26.
10. Arikawa K, Molday LL, Molday RS, Williams DS. Localization of peripherin/rds in the disk membranes of cone and rod photoreceptors: relationship to disk membrane morphogenesis and retinal degeneration. *J Cell Biol*. 1992;116:659–667.
11. Chang HY, Ready DF. Rescue of photoreceptor degeneration in rhodopsin-null Drosophila mutants by activated Rac1. *Science*. 2000;290:1978–1980.
12. Ridley AJ, Paterson HF, Johnston CL, Diekmann D, Hall A. The small GTP-binding protein rac regulates growth factor-induced membrane ruffling. *Cell*. 1992;70:401–410.
13. Ridley AJ. Rho GTPases and actin dynamics in membrane protrusions and vesicle trafficking. *Trends Cell Biol*. 2006;16:522–529.
14. Etienne-Manneville S, Hall A. Rho GTPases in cell biology. *Nature*. 2002;420:629–635.
15. Jaffe AB, Hall A. Rho GTPases: biochemistry and biology. *Annu Rev Cell Dev Biol*. 2005;21:247–269.
16. Heasman SJ, Ridley AJ. Mammalian Rho GTPases: new insights into their functions from in vivo studies. *Nat Rev Mol Cell Biol*. 2008;9:690–701.
17. Deretic D, Traverso V, Parkins N, et al. Phosphoinositides, ezrin/moesin, and rac1 regulate fusion of rhodopsin transport carriers in retinal photoreceptors. *Mol Biol Cell*. 2004;15:359–370.
18. Mitchell DC, Bryan BA, Liu JP, et al. Developmental expression of three small GTPases in the mouse eye. *Mol Vis*. 2007;13:1144–1153.
19. Balasubramanian N, Slepak VZ. Light-mediated activation of Rac-1 in photoreceptor outer segments. *Curr Biol*. 2003;13:1306–1310.
20. Belmonte MA, Santos MF, Kihara AH, Yan CY, Hamassaki DE. Light-induced photoreceptor degeneration in the mouse involves activation of the small GTPase Rac1. *Invest Ophthalmol Vis Sci*. 2006;47:1193–1200.
21. Haruta M, Bush RA, Kjellstrom S, et al. Depleting Rac1 in mouse rod photoreceptors protects them from photo-oxidative stress without affecting their structure or function. *Proc Natl Acad Sci U S A*. 2009;106:9397–9402.
22. Diekmann D, Brill S, Garrett MD, et al. *Bcr* encodes a GTPase-activating protein for p21*rac*. *Nature*. 1991;351:400–402.
23. Lem J, Applebury ML, Falk JD, Flannery JG, Simon MI. Tissue-specific and developmental regulation of rod opsin chimeric genes in transgenic mice. *Neuron*. 1991;6:201–210.
24. Belcastro M, Song H, Sinha S, et al. Phosphorylation of phosducin accelerates rod recovery from transducin translocation. *Invest Ophthalmol Vis Sci*. 2012;53:3084–3091.
25. Kjellstrom S, Bush RA, Zeng Y, Takada Y, Sieving PA. Retinoschisin gene therapy and natural history in the *Rs1h*-KO mouse: long-term rescue from retinal degeneration. *Invest Ophthalmol Vis Sci*. 2007;48:3837–3845.
26. Rich KA, Zhan Y, Blanks JC. Migration and synaptogenesis of cone photoreceptors in the developing mouse retina. *J Comp Neurol*. 1997;388:47–63.
27. Wei X, Malicki J. *nagie oko*, encoding a MAGUK-family protein, is essential for cellular patterning of the retina. *Nat Genet*. 2002;31:150–157.
28. Masai I, Lele Z, Yamaguchi M, et al. N-cadherin mediates retinal lamination, maintenance of forebrain compartments and patterning of retinal neurites. *Development*. 2003;130:2479–2494.
29. Malicki J. Cell fate decisions and patterning in the vertebrate retina: the importance of timing, asymmetry, polarity and waves. *Curr Opin Neurobiol*. 2004;14:15–21.
30. Koike C, Nishida A, Akimoto K, et al. Function of atypical protein kinase C lambda in differentiating photoreceptors is required for proper lamination of mouse retina. *J Neurosci*. 2005;25:10290–10298.
31. Cho SH, Kim JY, Simons DL, et al. Genetic ablation of *Pals1* in retinal progenitor cells models the retinal pathology of Leber congenital amaurosis. *Hum Mol Genet*. 2012;21:2663–2676.
32. Young RW. Cell differentiation in the retina of the mouse. *Anat Rec*. 1985;212:199–205.

Investigative Ophthalmology & Visual Science

33. Nam SC, Choi KW. Interaction of Par-6 and Crumbs complexes is essential for photoreceptor morphogenesis in Drosophila. *Development*. 2003;130:4363–4372.
34. Lin D, Edwards AS, Fawcett JP, et al. A mammalian PAR-3-PAR-6 complex implicated in Cdc42/Rac1 and aPKC signalling and cell polarity. *Nat Cell Biol*. 2000;2:540–547.
35. Qiu RG, Abo A, Steven Martin G. A human homolog of the *C. elegans* polarity determinant Par-6 links Rac and Cdc42 to PKCzeta signaling and cell transformation. *Curr Biol*. 2000;10: 697–707.
36. Henrique D, Schweisguth F. Cell polarity: the ups and downs of the Par6/aPKC complex. *Curr Opin Genet Dev*. 2003;13: 341–350.
37. Goldstein B, Macara IG. The PAR proteins: fundamental players in animal cell polarization. *Dev Cell*. 2007;13:609–622.
38. Petronczki M, Knoblich JA. DmPAR-6 directs epithelial polarity and asymmetric cell division of neuroblasts in Drosophila. *Nat Cell Biol*. 2001;3:43–49.
39. Suzuki A, Yamanaka T, Hirose T, et al. Atypical protein kinase C is involved in the evolutionarily conserved par protein complex and plays a critical role in establishing epithelia-specific junctional structures. *J Cell Biol*. 2001;152:1183–1196.
40. Wodarz A, Ramrath A, Grimm A, Knust E. Drosophila atypical protein kinase C associates with Bazooka and controls polarity of epithelia and neuroblasts. *J Cell Biol*. 2000;150:1361–1374.
41. Manabe N, Hirai S, Imai F, et al. Association of ASIP/mPAR-3 with adherens junctions of mouse neuroepithelial cells. *Dev Dyn*. 2002;225:61–69.
42. Whited JL, Cassell A, Brouillette M, Garrity PA. Dynactin is required to maintain nuclear position within postmitotic Drosophila photoreceptor neurons. *Development*. 2004;131: 4677–4686.
43. Tsujikawa M, Omori Y, Biyanwila J, Malicki J. Mechanism of positioning the cell nucleus in vertebrate photoreceptors. *Proc Natl Acad Sci U S A*. 2007;104:14819–14824.
44. Hale IL, Fisher SK, Matsumoto B. The actin network in the ciliary stalk of photoreceptors functions in the generation of new outer segment discs. *J Comp Neurol*. 1996;376:128–142.
45. Pellikka M, Tanentzapf G, Pinto M, et al. Crumbs, the Drosophila homologue of human CRB1/RP12, is essential for photoreceptor morphogenesis. *Nature*. 2002;416:143–149.
46. Mehalow AK, Kameya S, Smith RS, et al. CRB1 is essential for external limiting membrane integrity and photoreceptor morphogenesis in the mammalian retina. *Hum Mol Genet*. 2003;12:2179–2189.
47. Park B, Alves CH, Lundvig DM, et al. PALS1 is essential for retinal pigment epithelium structure and neural retina stratification. *J Neurosci*. 2011;31:17230–17241.
48. Izumi Y, Hirose T, Tamai Y, et al. An atypical PKC directly associates and colocalizes at the epithelial tight junction with ASIP, a mammalian homologue of *Caenorhabditis elegans* polarity protein PAR-3. *J Cell Biol*. 1998;143:95–106.
49. Joberty G, Petersen C, Gao L, Macara IG. The cell-polarity protein Par6 links Par3 and atypical protein kinase C to Cdc42. *Nat Cell Biol*. 2000;2:531–539.
50. Alves CH, Sanz AS, Park B, et al. Loss of CRB2 in the mouse retina mimics human retinitis pigmentosa due to mutations in the *CRB1* gene. *Hum Mol Genet*. 2013;22:35–50.
51. Bulgakova NA, Knust E. The Crumbs complex: from epithelial-cell polarity to retinal degeneration. *J Cell Sci*. 2009;122:2587–2596.
52. Chartier FJ, Hardy EJ, Laprise P. Crumbs controls epithelial integrity by inhibiting Rac1 and PI3K. *J Cell Sci*. 2011;124: 3393–3398.
53. Yamanaka T, Horikoshi Y, Suzuki A, et al. PAR-6 regulates aPKC activity in a novel way and mediates cell-cell contact-induced formation of the epithelial junctional complex. *Genes Cells*. 2001;6:721–731.
54. Young RW. Cell death during differentiation of the retina in the mouse. *J Comp Neurol*. 1984;229:362–373.
55. Satoh M, Ogita H, Takeshita K, et al. Requirement of Rac1 in the development of cardiac hypertrophy. *Proc Natl Acad Sci U S A*. 2006;103:7432–7437.
56. Brown GC. Mechanisms of inflammatory neurodegeneration: iNOS and NADPH oxidase. *Biochem Soc Trans*. 2007;35: 1119–1121.
57. Takada Y, Fariss RN, Tanikawa A, et al. A retinal neuronal developmental wave of retinoschisin expression begins in ganglion cells during layer formation. *Invest Ophthalmol Vis Sci*. 2004;45:3302–3312.

Investigative Ophthalmology & Visual Science